FACTA UNIVERSITATIS
Series: **Architecture and Civil Engineering** ONLINE FIRST
https://doi.org/10.2298/FUACE250331002M

Original Scientific Paper

REVIEW OF THE POTENTIALS FOR QUANTITATIVE MICROSTRUCTURAL ANALYSIS OF POLYMER-MODIFIED BITUMEN

UDC 691.16

Miomir Miljković

University of Niš, Faculty of Civil Engineering and Architecture, Niš, Serbia

ORCID iDs: Miomir Miljković https://orcid.org/0000-0002-1821-4651

Abstract. *The objective of this article is to provide a critical synthesis and review of the potentials of the most relevant techniques and analysis procedures for styrene-butadiene-styrene (SBS)- and epoxy-modified bitumen based on fluorescence microscopy. This analysis considers SBS-modified bitumens with the mass fractions of SBS from 1.5 to 6 % and epoxy-modified bitumens with 10 to 90 % of epoxy. The content of polymeric phases plays a main role in the morphological characteristics and the percolation of microstructure. The SBS-modified bitumen shows a tendency towards distortion of droplet shapes into complex microencapsulated structures, thus significantly increasing particle's bulk volume. This also seriously questions the assumption of continuum used in the linear viscoelastic testing and modelling. The microstructure of the epoxy-modified bitumen gradually evolved from an even dispersion of epoxy droplets to almost bimodal dispersion of bituminous particles within epoxy. By approaching the phase inversion, epoxy gradually encapsulates bituminous nuclei. Future research should focus on how microstructure affects the non-linear viscoelasticity of bitumen, especially regarding the formation of large polymeric agglomerations. Besides, an involvement of infrared microscopy is critical for understanding the interfacial chemical interactions of polymer and residual bitumen.*

Key words: *polymer-modified bitumen, styrene-butadiene-styrene (SBS), epoxy resin, fluorescence microscopy, microstructure, morphology*

1. INTRODUCTION

The contemporary scientific development of asphalt science, especially form the aspect of bitumen modification, inevitably introduced more sophisticated and fundamental methods for experimental evaluation and computational analysis of bitumen's microstructure.

Received March 31, 2025 / Revised April 23, 2025 / Accepted April 24, 2025
Corresponding author: University of Niš, Faculty of Civil Engineering and Architecture
Aleksandra Medvedeva 14, 18000 Niš, Serbia
E-mail: miomir.miljkovic@outlook.com

© 2025 by University of Niš, Serbia | Creative Commons License: CC BY-NC-ND

This advancement essentially fosters deeper scientific understanding and interpretation of material's behaviour as well as its macroscopic performance. The application of various microscopic techniques [1] aims to provide an insight in how different external impacts are manifested across different length scales of asphalt down to bitumen's internal structure. Although, fluorescence microscopy has been extensively used for the evaluation of microstructure of polymer-modified bitumen, the compatibility between the polymer and base bitumen, as well as for assessment of the homogeneity of their blend, quantitative characterisation of the morphology and topology has been barely introduced for both scientific and practical purposes. For this reason, a systematic quantification of the microstructural features, including the kinetics of their evolution over time is critical to link the bitumen's chemical composition with its conventionally evaluated rheological properties. Since both bitumen and polymer are phases which undergo percolation in the critical domains of blend composition, temperature, shear stress state, and other, they can both experience phase inversion. Consequently, the system can consist of both discrete particles and continuous percolated entities, which stresses the importance to evaluate the most suitable approaches for the quantification of the morphology in both cases.

The most common solution to elastomeric polymer-modification of bitumen is the dispersion of styrene-butadiene-styrene (SBS). Nevertheless, simultaneously to its, generally positive, effect on the overall mechanical behaviour the micromorphology of SBS-modified bitumen can be quite dependent on conditions bitumen is subjected to. This especially refers to thermo-oxidative ageing and mixing during the process of production [2, 3]. An intrinsic component of such morphological variability is the percolation and depercolation of bitumen and SBS as main and quasidiscrete phases of the system. Regarding the volumetric composition, the above-mentioned conditions can result in the dispersion of SBS droplets within continuous bituminous phase or vice versa. Such potential evolution is confirmed to be directly reflected in bitumen's macroscopic mechanical properties [4].

The use of epoxy resins is another common type of modification of bitumen, where the interfacial morphology is even more influential because of a drastic difference between individual phases' thermo-mechanical response [5, 6]. Due to epoxy's much higher modulus of elasticity and much lower thermo-mechanical sensitivity, the understanding and ability to influence the epoxy-modified bitumen' microstructure is even more significant.

The variability and potential temporal evolution of the polymer-modified bitumen's microstructure is the major goal of the microscopic analysis of this material [7–11]. Therefore, the objective of this article is to provide a critical synthesis and review of the most relevant microscopic techniques and analysis procedures for polymer-modified bitumen. For this purpose, the fluorescence microscopy is considered as the most common approach. Besides, this consideration is focused on the SBS- and epoxy-based modifications as the most common modification approaches.

2. Materials and Methods

2.1. Materials

To review the effect of different initial volumetric compositions of bitumens, this analysis considers SBS-modified bitumens with the mass fractions of SBS of 1.5, 3, 4.5, and 6 %. Since the phase inversion phenomenon is typical for the optimisation of epoxy-modified bitumen's composition, bitumens with the mass fractions of 10 to 90 % of epoxy [1] are also considered. For both bitumens, blends and microscopy specimens are prepared by already well-established procedures [5, 6, 12]. Thus, the SBS-modified specimens are prepared by inducing fractured surfaces of deeply frozen specimens, while the epoxy-modified specimens are observed by placing a drop of the blend on a glass plate.

2.2. Postprocessing and analysis of images

2.2.1. Segmentation

The most important algorithms used in postprocessing original micrographs are the clustering of the histograms of grey values and the thresholding of the individual phases [13]. Where applicable, various algorithms for the reduction of imaging noise could also be applied, but this potentially results in a certain loss of details in original images.

2.2.2. Clustering and thresholding

The clustering operation groups the grey values of original images by applying the *k*-means algorithm, so the resulting groups (clusters) correspond to distinct physical phases. In the case of SBS-modified bitumen, three dominant phases can be distinguished from the histogram and correspond to the continuous bituminous phase (Phase 1), interfacial diffusion gradients (Phase 2), and SPS particles (Phase 3). The clustering algorithm determines grey values standing for the centres of individual clusters by minimising the mean squared distance of individual histogram values to the nearest centre [14–16]. The output clustered images are subjected to thresholding [16] to obtain the final binary images of the phases. All subsequent morphological analyses are performed on these thresholded binary images. The disposition of individual image phases in the case of SBS-modified bitumen [17] is shown in **Fig. 1**.

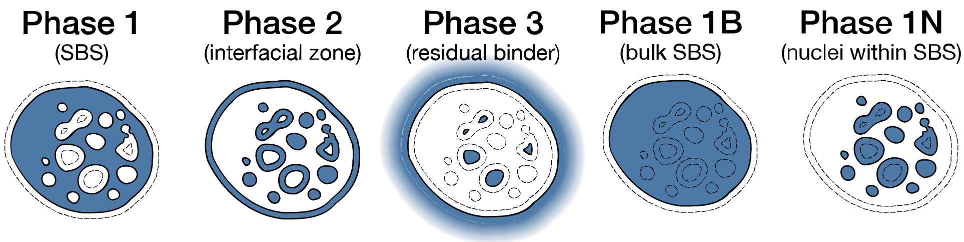

Fig. 1 Overview of phases segmented from the micrographs of SBS-modified bitumen and their physical interpretations

Nevertheless, it must be pointed out that the segmentation of all image phases only corresponds to the fluorescence properties of specimens. The analogy of these properties to the chemical compositions, and thus physical interpretations (polymer or bitumen in this case) is purely empirical. This is the reason why the image phases are designated by generic names (Phases 1, 2, …) rather than using their material interpretation [13].

2.2.3. Morphology of discrete particles

The size and shape of discrete entities of the thresholded binary images (referred to as particles) are characterised by the area-weighted cumulative distribution functions of particle areas. In addition to the distribution of particle areas, the particle shape is quantified by their circularity (measure of deviation from the round shape) and solidity (measure of convexity) [18].

2.2.4. Local thickness distribution

The characterisation of the morphological features of highly interconnected (networked) phases is done by determining their local thickness distributions [1, 19–22]. The local thickness distribution takes into account the phase's entire volume (are in the case of microscopy) without performing any disconnecting operation [13]. This algorithm successively applies morphological erosions and dilations [23]. The resulting subset areas are used to calculate the local thickness distribution as

$$\begin{gathered}
\varphi_{i,\mathrm{ED}}(r_j) \equiv \frac{A_{i,\mathrm{ED}}(r_j)}{A_i} = \frac{A_i - \sum_{k=1}^{j} \Delta A_{i,\mathrm{ED}}(r_k)}{A_i} = 1 - \frac{A_{i,\mathrm{cum}}(r_j)}{A_i} = 1 - \varphi_{i,\mathrm{cum}}(r_j) \\
r_j = j\,\Delta r \qquad j = 0,1,\dots,\left\lceil \frac{r_{\max}}{\Delta r} \right\rceil \\
\Delta A_{i,\mathrm{ED}}(r_k) = A_{i,\mathrm{ED}}\left[(k-1)\,\Delta r\right] - A_{i,\mathrm{ED}}(k\Delta r)
\end{gathered} \tag{1}$$

where φ_{ED} represents the area fraction of individual eroded and dilated entity with the radius r, i represents the index of phase, j represents the index of iteration, A_{ED} represents the area of the entity, A represents the total area of the given phase, A_{cum} represents the complementary area to A_{ED}, ΔA_{ED} represents the differential area, Δr represents the increment, and $r_{\max}$ represents the maximal radius. The principle of this analysis is shown in **Fig. 2**.

3. RESULTS

3.1. SBS-modified bitumen

The fluorescence micrographs of the SBS-modified bitumen [17] are shown in **Fig. 3** and Figure 4. It can be seen that the SBS content is a decisive factor for the morphology, as well as the topology, of the systems' internal structure. The most obvious effect is that higher content of SBS increases in the areas of individual SBS particles. In this regard, at the lowest SBS content bitumen is a homogeneous dispersion of polymer droplets. Nevertheless, at 3 % of SBS the polymer droplets begin to be encapsulated with characteristic shells around the nucleated bituminous phase. At 4.5 % of SBS, the system clearly became a polynuclear encapsulated dispersion with a considerable degree of inter-particle coalescence [24–26]. This process culminated for 6 % of SBS, but, even then, the bitumen obviously had no tendency to approach the phase inversion.

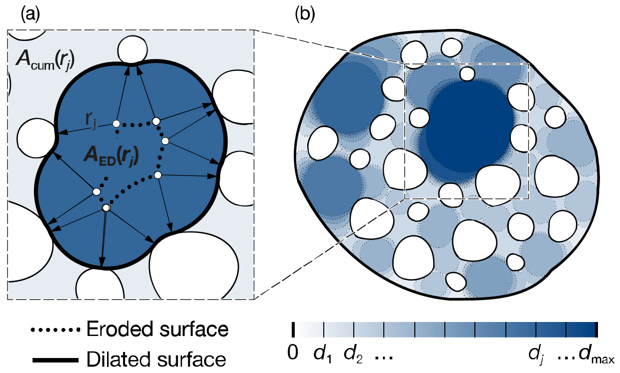

Fig. 2 Illustration of the general principle of the successive analysis of local thickness distribution: (a) successive operations of erosion and dilation as functions of radius and (b) output map of the local radii [1]

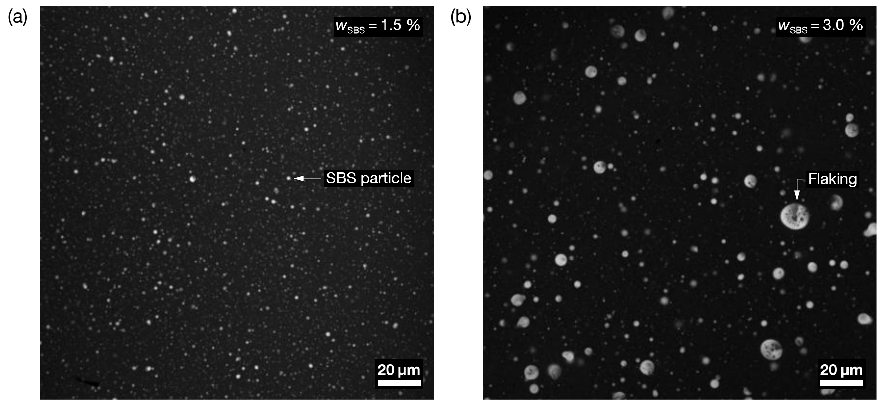

Fig. 3 Fluorescence micrographs of the SBS-modified bitumen: (a) 1.5 % of SBS, (b) 3.0 % of SBS

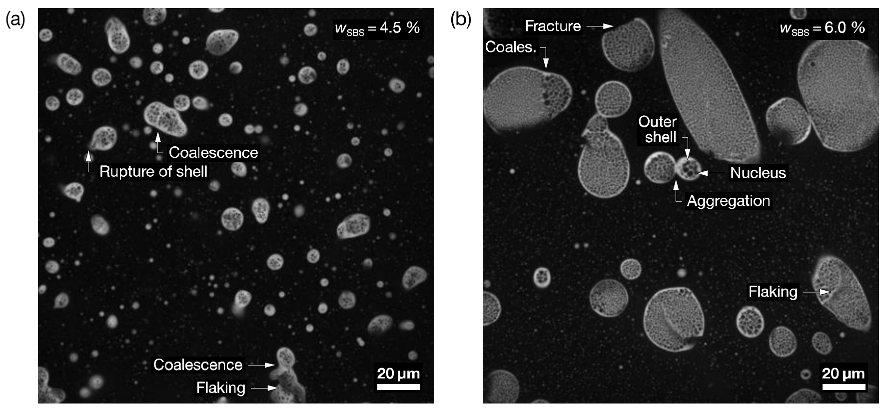

Fig. 4 Fluorescence micrographs of the highly SBS-modified bitumen: (a) 4.5 % of SBS, and (b) 6.0 % of SBS

The particle area, circularity, and solidity distribution of the main and supplementary phases are shown in Figures 5 to 7, respectively. The diagrams confirm the significant increase in particle areas with the SBS content, and such behaviour is consistently present in both Phases 1 and 1B. On the other hand, the areas of bituminous nuclei (Phase 1N) also increase considerably, but this trend stabilises as the highest SBS content is reached.

The circularity of individual SBS particles also increases with their area (i.e. mass fraction). Because of the mentioned nucleation process, the discrepancy with the results of Phases 1 and 1B became evident at 4.5 % of SBS. This evolution strongly distorts the shape of SBS particles at the highest content of SBS, and almost all larger particles are below the empirical limit of 0.5. As it is well-known from the previous research, the solidity is less sensitive to the content of SBS, and in almost all cases of SBS content, well above 0.5.

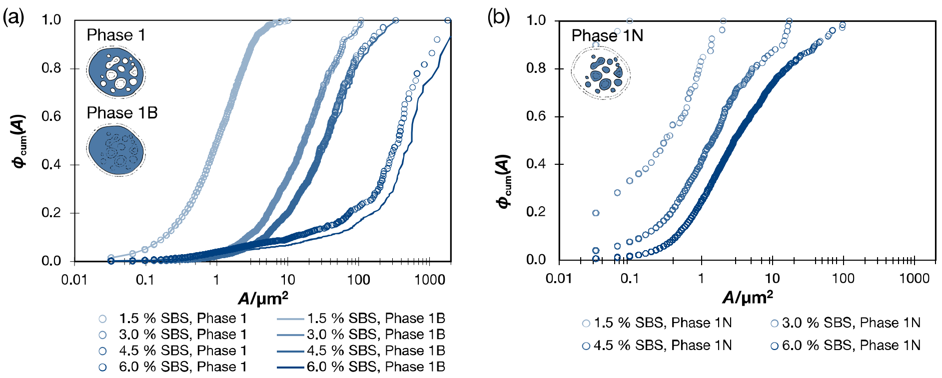

Fig. 5 Particle size distributions (cumulative area-weighted distributions as functions of particle area fractions): (a) Phase 1 corresponding to SBS droplets and Phase 1B corresponding to bulk SBS droplets, and (b) Phase 1N corresponding to the nuclei within SBS droplets [17]

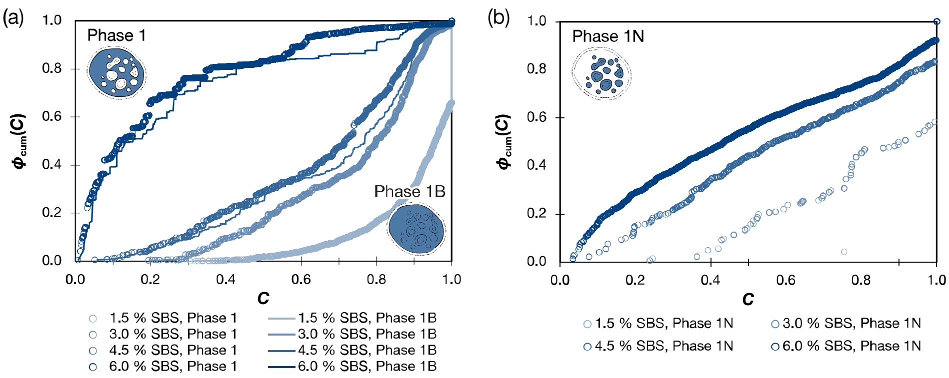

Fig. 6 Distributions of particle circularities (cumulative area-weighted distributions as functions of particle circularities): (a) Phase 1 corresponding to SBS droplets and Phase 1B corresponding to bulk SBS droplets, and (b) Phase 1N corresponding to the nuclei within SBS droplets [17]

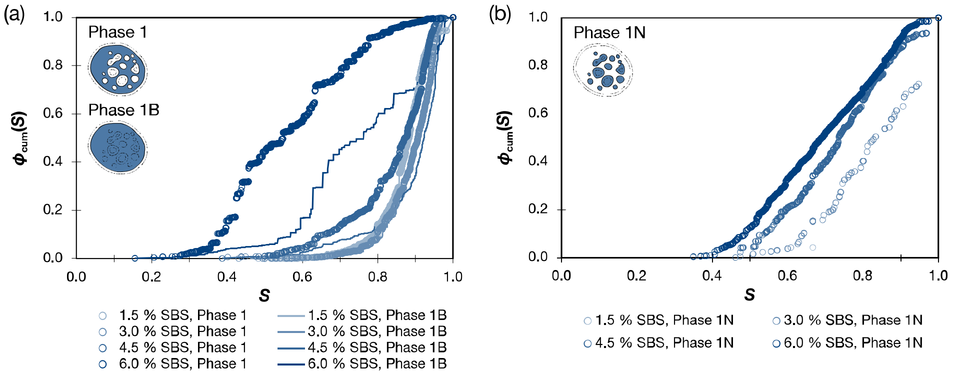

Fig. 7 Distributions of particle solidities (cumulative area-weighted distributions as functions of particle solidities): (a) Phase 1 corresponding to SBS droplets and Phase 1B corresponding to bulk SBS droplets, and (b) Phase 1N corresponding to the nuclei within SBS droplets [17]

3.2 Epoxy-modified bitumen

A original micrographs of epoxy-modified bitumen specimens [1] are shown in Fig. **9**. As simulated by the selection of initial volumetric compositions of these blends, it can be observed that the systems undergo a typical phase inversion with epoxy phase percolating (and bituminous phase depercolating) as the fraction of epoxy increases. Unlike SBS-modified bitumen, the distortion of epoxy droplet morphology (below the inversion point taking place in the range from 40 and 50 % of epoxy) is much less present. It is noticeable that, as the composition approaches the inversion, an extensive encapsulation of bituminous nuclei at 40 % of epoxy is the dominant mode of the system's destabilisation. Nevertheless, since the phase inversion itself apparently happens as a catastrophic event, such condition is not possible to capture with the given increment of the epoxy content.

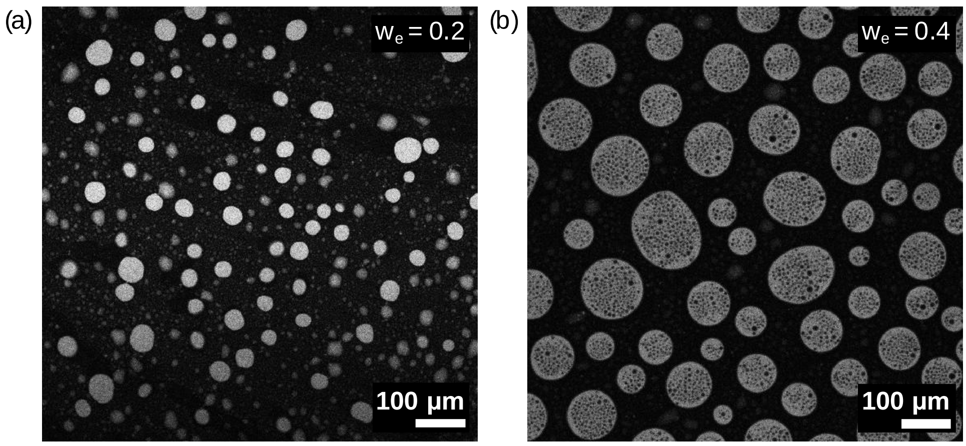

Fig. 8 Original fluorescence micrographs of the specimens with different mass fractions of epoxy, w_e: (a) w_e=20 %, (b) w_e=40 %

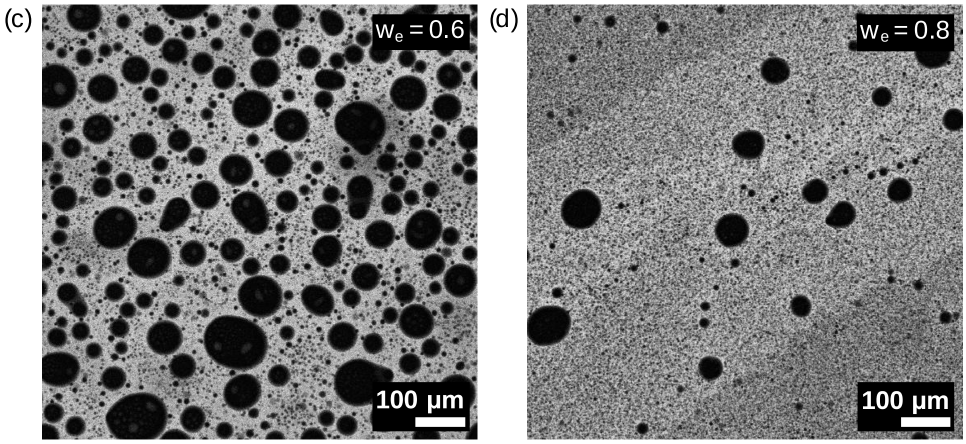

Fig. 9 Original fluorescence micrographs of the specimens with different mass fractions of epoxy, (c) w_e=60 %, and (d) w_e=80 %

Above the inversion point, the specimens transformed to a mostly homogeneous dispersion of bituminous droplets within the continuous epoxy matrix. As the content of epoxy approaches 90 %, the droplets' spatial distribution becomes less random with a considerable agglomeration of the smallest bitumen particles and their apparent merging (closely to the resolution limit). Such configuration shows a tendency towards a bimodal dispersion with highly constrained movability of droplets.

Since the blend with 40 % of epoxy represents the most complex case of the percolation of both phases, colour maps of its phases' local thickness distributions are shown in Figure 10 and 11.

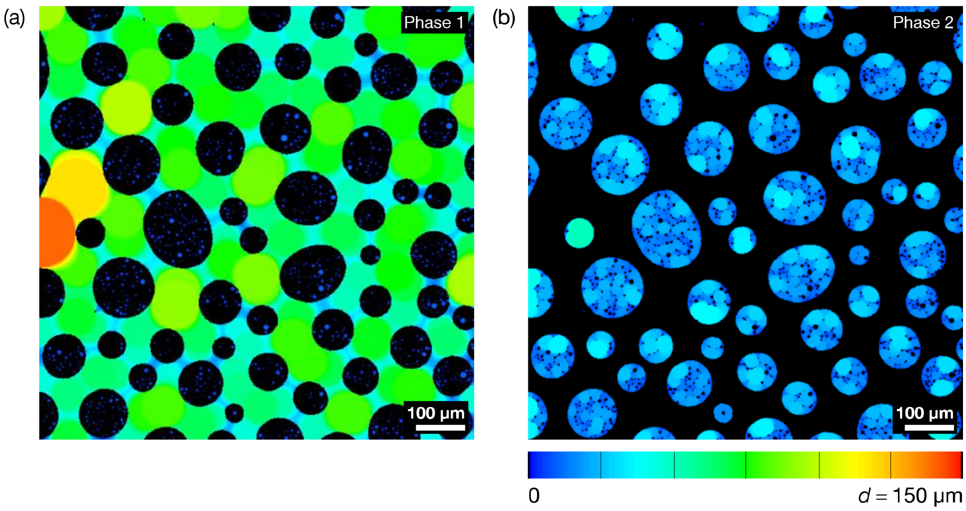

Fig. 10 Visualisation the local thickness distribution colour maps of Phases 1 and 2 at 40 % of epoxy: (a) Phase 1 (b) Phase 2 [1]

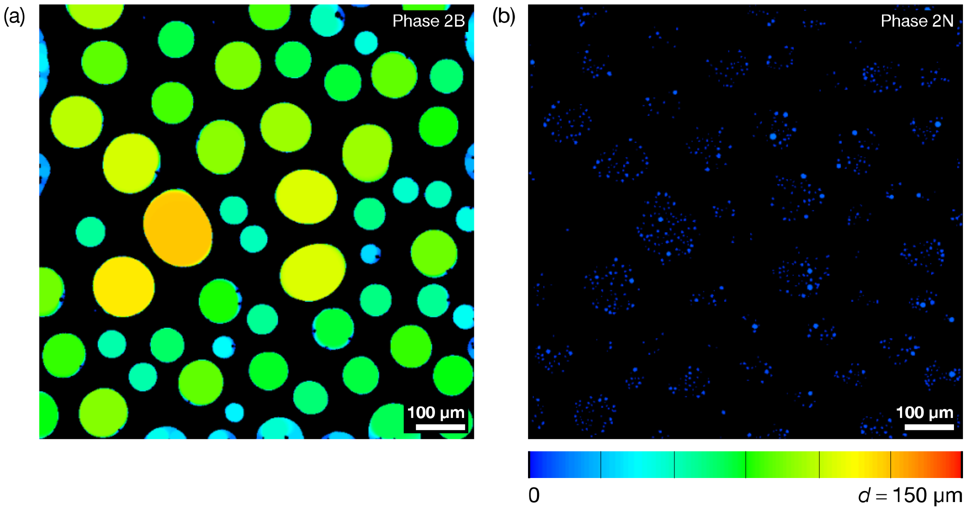

Fig. 11 Visualisation the local thickness distribution colour maps of Phases 2B and 2N at 40 % of epoxy: (a) Phase 2B and (b) Phase 2N [1]

The diagrams of these distributions of Phase 1 are shown in **Fig. 12**. It can be observed that the local thicknesses grow with the content of epoxy as epoxy droplets coalesce and grow in size. However, as both Phases 1 and 2 percolate into the characteristic networked topologies, the local thickness distributions drastically drop directly suggesting the lower bulk viscosity of epoxy polynuclear capsules.

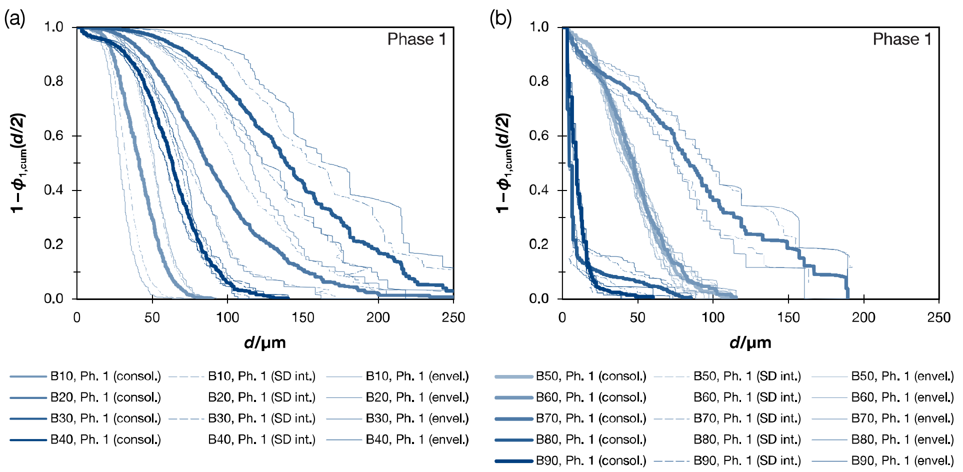

Fig. 12 Local thickness distributions of Phase 1 (combined samples and envelopes) for different mass fractions of epoxy: (a) pre-inversion domain (10 to 40 % of epoxy) and (b) post-inversion domain (50 to 90 % of epoxy) [1]

4. Conclusions

This article reviewed the potential for the quantitative micromorphological characterisation of polymer-modified bitumen with the application of SBS and epoxy based on fluorescence microscopic measurements. The analysis took into account the morphological parameters of size and shape of discrete particles (droplets), as well as the local thickness distribution of interconnected phases.

It can be concluded that the volume fraction of polymeric phases plays the main role in the morphological characteristics and the percolation process of the observed specimens. Moreover, the two considered polymers exhibit completely different microstructural behaviour. in this regard, SBS-modified bitumen shows a more prominent tendency towards distortion of droplet shapes into complex microencapsulated configurations with significant increase in particles bulk volume. Despite the fact that the chemical diffusion between the phases cannot be evaluated by the fluorescence microscopy, the nucleation of bitumen inside polymer is the underlying reason of the macroscopically observed phenomenon referred to as polymer swelling. Furthermore, the presence of large SBS structures seriously questions the assumption of continuum during the bitumen's linear viscoelastic testing (commonly by oscillatory shear).

It is confirmed that the microstructure of the epoxy-modified bitumen gradually evolved from a dispersion of spherical epoxy droplets evenly distributed throughout the bituminous phase to an almost bimodal dispersion of partially coalesced bituminous particles within an epoxy percolated matrix. The inversion of phases does not take place symmetrically around the inversion point. Thus, it is typical that a system approaching the inversion first gradually incorporates bituminous droplets inside epoxy (acting like a capsule), while the inversion itself happens within much narrower range of epoxy contents (possibly as a catastrophic event).

Although the available results provide lots of knowledge on how the microstructure affects the macroscopic rheological performance, there is still insufficient understanding on how the microstructure causes the mechanical non-linearity of specimens. Moreover, it is necessary to comprehensively investigate the potential effects of the formation large and heterogeneous polymeric structures on the validity of the hypothesised continuum in the calculation of mechanical variables from the rheological measurements.

Future research should explore the systems' behaviour closely to the domain of phase inversion which is necessary for the optimal design of composition of modified bitumen blends. An important subject for further work is the involvement of advanced infrared microscopic techniques to also obtain an insight into the chemical interactions at the interface between a polymer and residual bitumen. Consequently to the expected diffusion of light derivatives from bitumen into the polymer, the macromechanical manifestations of the residual bitumen's impaired mechanical properties are important to understand the compensation between positive and possibly negative roles of polymer modification on the micro scale.

REFERENCES

1. Miljković, M., Wu, C., Jelagin, D., and Xie, H., 2024. Microstructural analysis of the phase separation of epoxy-modified bitumen. Construction and Building Materials, 451,138596. https://doi.org/10.1016/j.conbuildmat.2024.138596
2. Long, K., Huang, C., Yang, Y., Qu, C., Huang, H., Ai, C., and Yan, C., 2025. Investigation of the rheological properties and aging performance of rock asphalt/thermoplastic polyurethane composite modified asphalt. Construction and Building Materials, 458, 139699. https://doi.org/10.1016/j.conbuildmat.2024.139699
3. Zhao, Y., Wu, X., Chao, Y., Liang, N., Zhou, P., Li, Z., and Mei, Y., 2024. Aging characteristics and microscopic mechanisms of SBS asphalt based on coupled light–heat–water aging. Construction and Building Materials, 456, 139190. https://doi.org/10.1016/j.conbuildmat.2024.139190
4. Zhu, X., Wang, Y., Miljković, M., Li, R., and Hao, G., 2024. Effects of polymer structure on the physicochemical and performance-related properties of SBS-modified asphalt binders subjected to short-term aging. Construction and Building Materials, 411, 134446. https://doi.org/10.1016/j.conbuildmat.2023.134446
5. Xie, H., Li, C., and Wang, Q., 2024. Thermosetting polymer modified asphalts: Current status and challenges. Polymer Reviews, 64 (2), 690–759. https://doi.org/10.1080/15583724.2023.2286706
6. Wu, C., Yang, H., Cui, X., Cai, J., Yuan, Z., Zhang, J., and Xie, H., 2024. Thermo-mechanical properties and phase-separated morphology of warm-mix epoxy asphalt binders with different epoxy resin concentrations. Molecules, 29 (14), 3251. https://doi.org/10.3390/molecules29143251
7. Li, F., Wang, Y., Miljković, M., Chan, K.M., 2022. Changes in the nanoscale asphaltene particles and relaxation spectra of asphalt binders during aging and rejuvenation. Materials and Design, 219, 110808. https://doi.org/10.1016/j.matdes.2022.110808
8. Zhu, X., Miljković, M., Wang, Y., Hao, G., 2023. Property transitions of neat and styrene-butadiene-styrene (SBS)-modified asphalt binders from small, medium to large-amplitude oscillatory shears. International Journal of Pavement Engineering, 24 (2), 2068548. https://doi.org/10.1080/10298436.2022.2068548
9. Zhu, X., Wang, Y., Miljković, M., Li, R., and Hao, G., 2024. Effects of polymer structure on the physicochemical and performance-related properties of SBS-modified asphalt binders subjected to short-term aging. Construction and Building Materials, 411, 134446. https://doi.org/10.1016/j.conbuildmat.2023.134446
10. Blom, J., Soenen, H., Katsiki, A., Van den Brande, N., Rahier, H., Van den bergh, W., 2018. Investigation of the bulk and surface microstructure of bitumen by atomic force microscopy. Construction and Building Materials, 177, 158–169. https://doi.org/10.1016/j.conbuildmat.2018.05.062
11. Blom, J., Soenen, H., Van den Brande, N., Van den bergh, W., 2021. New evidence on the origin of 'bee structures' on bitumen and oils, by atomic force microscopy (AFM) and confocal laser scanning microscopy (CLSM). Fuel, 303, 121265. https://doi.org/10.1016/j.fuel.2021.121265
12. Hao, G., and Wang, Y., 2021. 3D reconstruction of polymer phase in polymer-modified asphalt using confocal fluorescence microscopy. Journal of Materials in Civil Engineering, 33 (1), 04020400. https://doi.org/10.1061/(ASCE)MT.1943-5533.0003485
13. Miljković, M., Griffa, M., Münch, B., Plamondon, M., and Lura, P., 2024. Mesostructural evolution of fine-aggregate bitumen emulsion–cement composites by X-ray tomography. International Journal of Pavement Engineering, 25 (1), 2283610. https://doi.org/10.1080/10298436.2023.2283610
14. Kanungo, T., Mount, D.M., Netanyahu, N.S., Piatko, C.D., Silverman, R., and Wu A.Y., 2002. An efficient *k*-means clustering algorithm: analysis and implementation. IEEE Transactions on Pattern Analysis and Machine Intelligence, 24 (7), 881–892. https://doi.org/10.1109/TPAMI.2002.1017616
15. Hung, C.-C. and Enmin Lan, S.Y., 2019. Image Texture Analysis: Foundations, Models and Algorithms. Cham: Springer. https://doi.org/10.1007/978-3-030-13773-1
16. Distante, A. and Distante, C., 2020. Handbook of Image Processing and Computer Vision, Volume 2: From Image to Pattern. Cham: Springer. https://doi.org/10.1007/978-3-030-42374-2
17. Zhu, X., Miljković, M., Li, R., Hao, G., Chen, X., and Wang, Y., 2025. Non-linear viscoelastic and micromorphological properties of SBS-modified asphalt binder. Materials and Design (article in press), 113958. https://doi.org/10.1016/j.matdes.2025.113958
18. Distante, A. and Distante, C., 2020. Handbook of Image Processing and Computer Vision, Volume 1: From Energy to Image. Cham: Springer. https://doi.org/10.1007/978-3-030-38148-6
19. Münch, B. and Holzer, L., 2008. Contradicting Geometrical Concepts in Pore Size Analysis Attained with Electron Microscopy and Mercury Intrusion. Journal of the American Ceramic Society, 91 (12), 4059–4067. https://doi.org/10.1111/j.1551-2916.2008.02736.x
20. Holzer, L., Münch, B., Iwanschitz, B., Cantoni, M., Hocker, Th., and Graule, Th., 2011. Quantitative relationships between composition, particle size, triple phase boundary length and surface area in nickel-cermet anodes for Solid Oxide Fuel Cells. Journal of Power Sources, 196 (17), 7076–7089. https://doi.org/10.1016/j.jpowsour.2010.08.006

21. Holzer, L., Iwanschitz, B., Hocker, Th., Münch, B., Prestat, M., Wiedenmann, D., Vogt, U., Holtappels, P., Sfeir, J., Mai, A., and Graule, Th., 2011. Microstructure degradation of cermet anodes for solid oxide fuel cells: Quantification of nickel grain growth in dry and in humid atmospheres. Journal of Power Sources, 196 (3), 1279–1294. https://doi.org/10.1016/j.jpowsour.2010.08.017
22. Soille, P., 2004. Morphological Image Analysis: Principles and Applications. 2nd ed. Berlin Hamburg: Springer-Verlag. https://doi.org/10.1007/978-3-662-05088-0
23. Salager, J.-L., 2006. Emulsion Phase Inversion Phenomena. Emulsions and Emulsion Stability, 2nd Ed. Boca Raton: Taylor & Francis Group. https://doi.org/10.1201/9781420028089-8
24. Pawar, A.B., Caggioni, M., Hartel, R.W., Spicer, P.T., 2012. Arrested coalescence of viscoelastic droplets with internal microstructure. Faraday Discuss, 158 (1), 341–50. https://doi.org/10.1039/C2FD20029E
25. Xie, Z., Burke, C.J., Mbanga, B., Spicer, P.T., Atherton, T.J., 2019. Geometry and kinetics determine the microstructure in arrested coalescence of Pickering emulsion droplets. Soft Matter, 15 (46), 9587–9596. https://doi.org/10.1039/C9SM00435A
26. Matsuda, M., Hayashi, H., Garcia-Ojalvo, J., Yoshioka-Kobayashi, K., Kageyama, R., Yamanaka, Y., Ikeya, M., Toguchida, J., Alev, C., and Ebisuya, M., 2020. Species-specific segmentation clock periods are due to differential biochemical reaction speeds. Science, 369 (6510), 1450–1455. https://doi.org/10.1039/d2sm00063f

PREGLED POTENCIJALA ZA KVANTITATIVNU MIKROSTRUKTURNU ANALIZU POLIMERNO MODIFIKOVANOG BITUMENA

Predmet ovog rada je da pruži kritičku sintezu i pregled najrelevantnijih tehnika i postupaka analize bitumena modifikovanog stiren-butadijen-stirenom (SBS) i epoksidnim smolama na bazi fluorescentne mikroskopije. Analizom su obuhvaćeni SBS-modifikovani bitumeni sa masenim udelom SBS-a od 1.5 do 6 % i epoksidno modifikovani bitumeni sa 0 to 90 % SBS-a. sadržaj polimernih faza igra glavnu ulogu u morfološkom karakteristikama i perkolaciji mikrostrukture. SBS-modifikovani bitumen pokazuje tendenciju ka distorziji oblika kapljica u kompleksne mikroenkapsulirane strukture, tako značajno povećavajući ukupnu zapreminu čestica. Ovo ozbiljno dovodi u pitanje pretpostavku kontinuuma koja se koristi pri linearnom viskoelastičnom ispitivanju i modeliranju. Mikrostruktura epoksidno modifikovanog bitumena postepeno evoluira od homogene disperzije kapljica epoksida do skoro bimodalne disperzije čestica bitumena u okviru epoksida. Približavajući se inverziji faza, epoksid postepeno enkapsulira bitumenske nukleuse. Buduće istraživanje treba da se usredsredi na to kako se mikrostruktura odražava na nelinearnu viskoelastičnost bitumena, posebno s obzirom na formiranje krupnih polimernih aglomeracija. Pored toga, primena infracrvene mikroskopije se smatra kritičnom za razumevanje međufaznih hemijskih interakcija polimera i rezidualnog bitumena.

Ključne reči: *polimerno modifikovani bitumen, stiren-butadijen-stiren (SBS), epoksidna smola, fluorescentna mikroskopija, mikrostruktura, morfologija*